



3D Printed Electronics of Non-contact Ink Writing Techniques: Status and Promise

Haining Zhang¹ · Seung Ki Moon¹ · Teck Hui Ngo²

Received: 11 October 2018 / Revised: 3 July 2019 / Accepted: 8 July 2019
© Korean Society for Precision Engineering 2019

Abstract

Non-contact ink writing techniques are a newly developed three-dimensional printing technology to fabricate customized and flexible electronic devices, while dramatically reducing chemical waste and lowering manufacturing costs. However, the use of non-contact ink writing technologies for fabricating electronics is still limited due to printing quality. To develop an electronic device with high performance, conductive lines should be printed with high controllability and excellent uniformity. Under such circumstances, many traditional optimization methods have been proposed to improve the printing quality. However, as the non-contact ink writing process is very sensitive to the system drifts and random variations, in situ process monitoring and online optimization technologies to optimize the printed line quality are in demand for practical printing. In this paper, we describe the processes of non-contact ink writing techniques based on inkjet printing (IJP) and aerosol jet printing (AJP). The key influencing factors in the non-contact ink writing processes are also discussed based on the three main printing stages. Then we analyze the advantages and disadvantages of the IJP and AJP techniques and review the state of art in quality optimization and precise control techniques that can be adopted in non-contact ink writing process. Additionally, to further develop a non-contact ink writing system, the major challenges and limitations of the current printing quality optimization technologies are also highlighted in this paper.

Keywords 3D printed electronics · Additive manufacturing · In situ process monitoring · Non-contact printing · Printing quality optimization

1 Introduction

A printed electronics technology is a newly developed 3D printing technology to produce flexible and low-cost device applications, such as customized diodes [1, 2], solar cells [3, 4], radio frequency identification tags (RFID) [5, 6], transistors [7–9] and sensors [10–12]. Compared with conventional approaches [13–15], a printable technology can significantly reduce fabrication process steps and chemical waste, while lowering fabrication costs. The two primary techniques for developing a printing system are contact printing and non-contact printing [16–20]. Different from the contact printing, a non-contact printing technology is maskless, and can print

with higher resolution and less waste, thus it has attracted great attention in various fields [21, 22]. Recently, there has been increasing interest in using the non-contact printing technology [23–25], especially ink-based inkjet printing (IJP) and aerosol jet printing (AJP) for printing electronic devices, semiconductors, and circuits, including thin-film transistors [18, 26, 27], light-emitting devices [28–30], sensors [31–34] and solar cells [35–38].

Despite non-contact printing possessing with many advantages [20, 39–42], the use of a non-contact ink writing technology for fabricating electronics is still limited due to printing quality [43–46]. As an important element of printed electronic devices, conductive lines should be printed with high controllability and excellent uniformity, thus Morphology Control (MC) and Uniformity Control (UC) are keys to fulfill these requirements [30, 47–50]. In addition to printing a straight line without bulging and scallop patterns, MC also refers to the capability of precise control over the printed line width in real time, while UC refers to the post-printing techniques used to suppress the coffee ring effect

✉ Seung Ki Moon
skmoon@ntu.edu.sg

¹ School of Mechanical and Aerospace, Nanyang Technological University, Singapore 639798, Singapore

² SMRT Corporation Ltd, Singapore 579828, Singapore

and improve the line uniformity of cross-sectional area [51]. Thus, MC and UC can be also classified as online and offline optimization, respectively.

In the non-contact ink writing technology, as identifying the correlations between the influencing factors and printed line morphology remains a challenge, most designers rely on personal experience for customized line width printing. Such manual and empirical operational approaches are imprecise and inefficient, as the lack of systematic and intelligent techniques to control the printed line morphology. Moreover, as the changes in material properties and a print head during printing, an ink writing system has an uncontrollable tendency to drift [47, 52], thus any empirical or theoretical models that correlate the process parameters to the line morphology should be calibrated before use for subsequent printing. If a high controllability over the line morphology is required, a real time and in situ monitoring technology is indispensable to ensure the printing process remain stable [47, 53]. Therefore, it is advantageous to adopt an in situ process monitoring and online optimization approach to detect process drifts and compensate the random variations. On the other hand, the coffee ring effect will cause non-uniform distribution of nanoparticles around the cross-sectional area, thus the lines are printed inhomogeneous and prevented from being widely applied to various electronic components which require excellent performance [45, 51]. Hence, UC is important to tune the relative distribution of nanoparticles around the cross-sectional area and improve the line conductivity. Therefore, online MC and offline UC are critical for the optimization of non-contact ink writing processes. As the printed line morphology should be optimized in a real-time situation and has direct impact on the line uniformity, MC is considered as the primary challenge in the optimization processes. Moreover, the relationship between different influencing factors and the printed line morphology is also highlighted to achieve MC.

In this paper, we review the processes of non-contact ink writing techniques based on IJP and AJP. The key influencing factors in the printing processes are discussed based on the printing stages. And, then different traditional approaches for printing quality optimization in IJP and AJP are reviewed with the advantages and disadvantages, and requirements for in situ monitoring and online optimization are subsequently highlighted. Finally, the progress of current real time and in situ monitoring technologies for online morphology control is reviewed and compared with the traditional approaches. In addition, the requirements and challenges of the current printing quality optimization technologies are also highlighted to further develop a non-contact ink writing system in this paper.

This paper is organized as follows: Sect. 2 provides an overview of the main non-contact ink writing processes including IJP and AJP. Section 3 discusses the critical

influencing factors on printing quality based on the different stages of non-contact ink writing. Section 4 presents a comprehensive review on traditional offline printing quality optimization approaches for non-contact ink writing process. Section 5 reviews the in situ monitoring and online optimization technologies for MC of the non-contact ink writing processes. In Sect. 6, the paper is concluded by providing an overview of the printing quality optimization approaches for the non-contact ink writing processes, and highlight the limitations of the current printing quality optimization technologies.

2 Non-contact Ink Writing Processes

2.1 Inkjet Printing

Based on different printing principles, IJP consists of two main types: a continuous inkjet (CIJ) printing system and a drop-on-demand (DoD) printing system [54–56]. The principle of the droplet formation and ejection is extremely different between these two print systems [57, 58]. As shown in Fig. 1a, a continuously flowing jet of the CIJ system can be controlled and broken up into uniform stream of droplets by a regular disturbance (such as a piezoelectric transducer), then for binary CIJ, the ink droplets are either charged or uncharged in an electric field. Eventually, the uncharged ink droplets impinge onto a substrate while the charged ink droplets are deflected and captured by the gutter for reuse.

In the DoD system as shown in Fig. 1b, a rapid change in the cavity volume is generated by an actuator. As the momentum imparts to the ejected droplet, single droplet will be activated and ejected by the print head. The subcategory of a DoD system is defined by the ink ejection mechanism of the nozzle: the piezoelectric, the electrostatic, the thermal, and the acoustic. As the capability of printing with higher spatial resolution and producing less contamination/waste than the CIJ system, the DoD systems are adopted in most research and discussed for printing electronics in this paper.

2.2 Aerosol Jet Printing

Compared with IJP, AJP is a newly developed technology for fabricating electronic components on both flat and non-flat substrates. In this technique, an atomizer (pneumatic or ultrasonic) is utilized to atomize the functional ink, and the generated aerosol of 2 to 5 μm (diameter) droplets is transported to the print head by a carrier gas flow. The entrained ink aerosol is then enwrapped by a sheath gas flow in the print head cylindrically. Due to the aerodynamic interaction between the sheath gas stream and the carrier gas stream, the aerosol droplets exits the nozzle tip and impacts the moving substrate with high speed, thus a line with high density

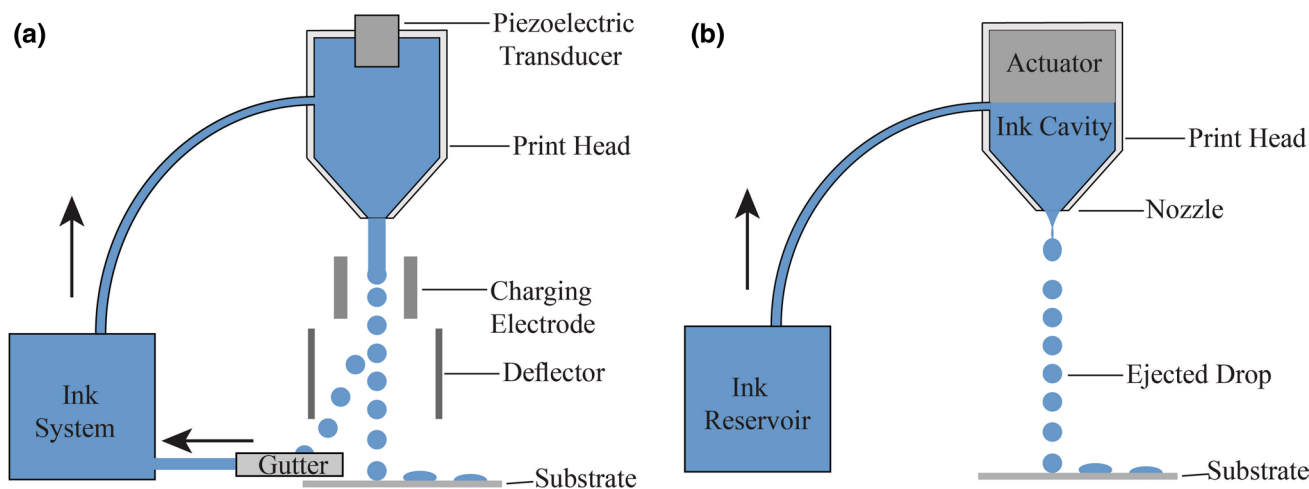


Fig. 1 Schematic diagram of a continuous inkjet printer, b drop-on-demand printer

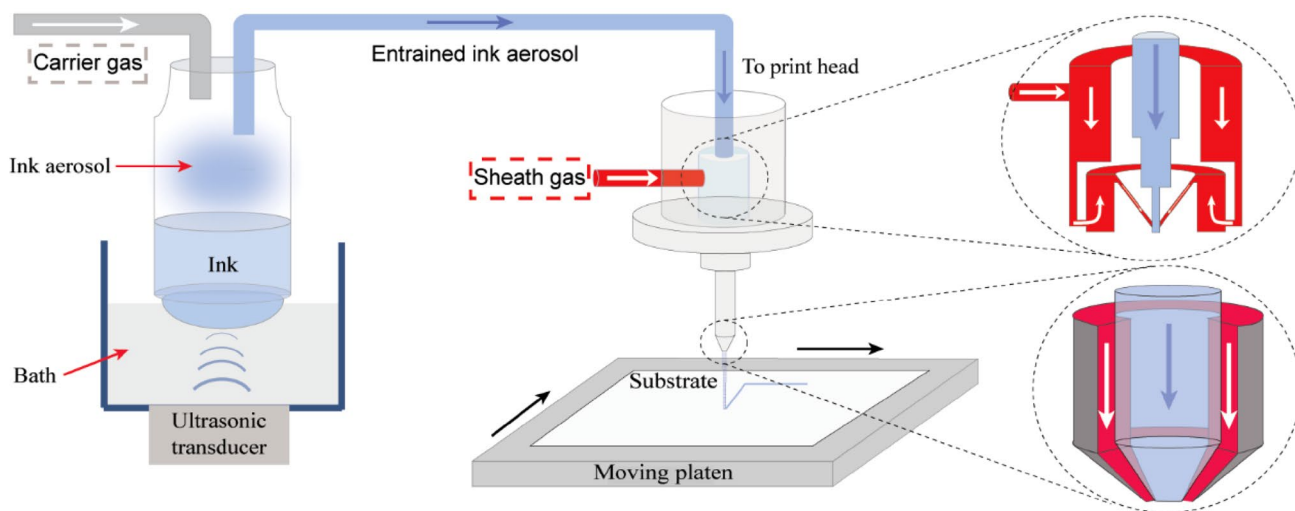


Fig. 2 Schematic of the aerosol jet printing process using an ultrasonic atomizer

and high resolution (down to the order of 10 μm) is fabricated on the substrate (about 2–5 mm below the nozzle tip). Figure 2 shows the working principles of the AJP process using an ultrasonic atomizer. The printed line morphology (width, thickness, roughness) is influenced significantly by the sheath gas flow rate (SHGFR), carrier gas flow rate (CGFR) and print speed, and the substrate could be heated to evaporate deposited solvents during the printing process.

2.3 The Comparison Between IJP and AJP

The comparison of basic technical specifications between IJP and AJP are shown in Table 1 [47, 57]. Despite the relatively lower print speed, AJP has flexible working height (1–5 mm), and is capable of printing high viscosity (1–2500 cP) functional ink over nonplanar substrates with

Table 1 Comparison of non-contact printing techniques

Characteristic	IJP	AJP
Printing principle	Electrostatic	Aerodynamic
Tip diameter (μm)	10–50	100–300
Tip height (mm)	1	1–5
Ink viscosity (cP)	10–20	1–2500
Process velocity (mm/s)	Up to 5000	Up to 200
Dynamic accuracy (μm)	N/A	± 6
Droplet size (pl)	1–8	0.001–0.005
Line thickness (nm)	5–500	100–5000
Particle diameter (nm)	< 100	10–700
Feature size (μm)	> 30	10–200
Surface tension (mN/m)	< 60	< 30
Metal loading (wt.%)	< 20	> 60
Throughput (m ² /s)	0.01–0.5	0.01–0.5

higher resolution (10 μm) and without clogging [21, 59–64]. However, to improve printing quality, it is necessary to further identify optimal operating windows based on the basic technical specifications that required by IJP and AJP.

3 Key Influencing Factors in Printing Process

To achieve better morphology control and uniformity assurance in non-contact ink writing processes, it is critical to identify the relationships between the adjustable factors and the line morphology in real time, and optimize the sintering process offline.

As shown in Fig. 3, the printing processes for the non-contact ink writing consist of three stages and the printed line morphology is the outcome of interaction between pre-printing factors and process parameters. Despite an empirical or theoretical model could correlate parts of factors to a printed line morphology, to accurately control the printed line morphology in real time, it is necessary to investigate the interactions between the adjustable factors in a design space systematically. And the design space could be explored by a data-driven based approach, which will be beneficial to study the influence of the two stages and model the correlations between the adjustable parameters and the printed line morphology for morphology control. Despite having many other effective approaches to restrain the coffee ring effect and improve the line uniformity, such as reducing the influence of outward capillary flow, producing a Marangoni flow,

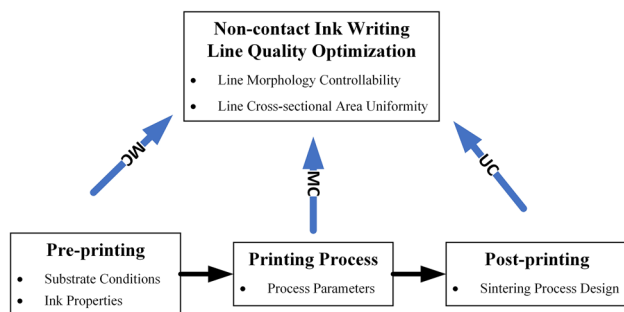


Fig. 3 Correlations between different printing stages and printed line quality

and developing patterned substrates [50, 65, 66], a practical way is to optimize the sintering process for the post-printing stage [45].

Based on the discussion above, the influencing factors of the printed line quality can be grouped into three main types: (1) pre-printing factors, (2) printing process parameters, and (3) post-printing factors as listed in Table 2. And, the printed line morphology is considered as a primary response to be optimized in this paper.

4 Traditional Printing Quality Optimization Approaches in Non-contact Ink Writing Processes

This section reviews the research works related to the printing quality optimization in IJP and AJP. For each printing technique, the traditional offline quality optimization approaches are discussed with the advantages and limitations, and requirements for in situ monitoring and online optimization are subsequently highlighted and proposed.

4.1 Inkjet Printing Process

As the application for printing electronics has been restricted by the ink printability of IJP [83], the behavior of liquid drops is selected to investigate the ink printability in many researches. To promote the printing controllability in droplet position and volume [78], an operability window as shown in Fig. 4 could be identified that allowed stable printing without splashing and satellite droplets. Under specific conditions, Fromm [84] proposed the value Z to determine the operability window of a functional ink in a DoD system, and $Z > 2$ was required to print single liquid droplet without satellites.

$$Z = \frac{(\gamma \rho a)^{1/2}}{\eta} \quad (1)$$

where η , ρ and γ is viscosity, density of the fluid and surface tension respectively, and a is a characteristic dimension (the radius of the tip size). Reis and Derby [85] further found that

Table 2 Influencing factors of ink writing processes

Categories	Influencing factors
Pre-printing factors [30, 48, 67–77]	Surface wettability, contact angle, ink viscosity, ink concentration, density, particle size, substrate temperature, surface tension
Process parameters [43, 44, 47, 48, 53, 60, 62, 71, 78–81]	IJP: droplet spacing, jetting delay, voltage, waveform, nozzle size, printing height AJP: SHGFR, CGFR, print speed, tip size, atomizer current, working height
Post-printing factors [45, 50, 76, 82]	Sintering temperature, sintering time, temperature gradient

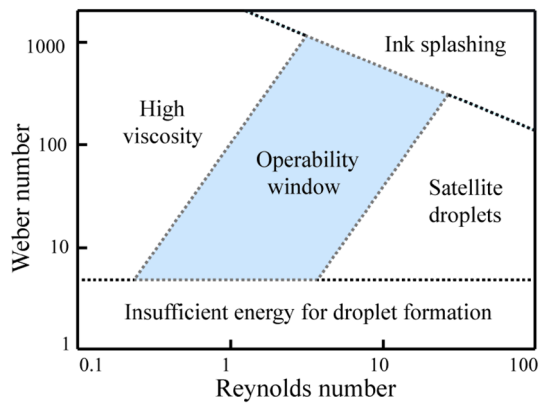


Fig. 4 Illustration of an operability window with respect to fluid properties for DOD inkjet printing

$1 < Z < 10$ was required for a printable fluid in most DoD printing systems.

However, different from the assumption of linear Newtonian fluid behavior in the aforementioned studies, the ink rheological properties in many applications for printing electronics are highly nonlinear, thus the printability window may need to be further modified [67]. Despite Jang et al. [68] considered different ink properties and defined the ink printability as $4 < Z < 14$ experimentally, $Z > 14$ [69, 70, 86–89] and $1 < Z < 4$ [68, 90, 91] were also found as printable range by many research groups for stable IJP, which means the process parameters of IJP, such as operating voltage, waveform and pulse width could also influence the droplet formation greatly. Therefore, to improve the printability of low viscosity fluids, some groups considered the interaction between the process parameters and the ink properties, and the key process factors for optimal droplet ejection were identified and the operating window for printing without satellites was further expanded [71, 72, 78, 79, 92]. Besides the printability, identifying the optimal process parameters by experimentation [46, 73, 74, 93] or modeling [75, 80] are also advantageous to further improve the resolution of printed droplets. However, the precise control over droplet size and size variation is more in demand for robust fabrication of inkjet printing. Chen et al. designed an inkjet printing system with capillary electrophoresis, hence the droplet volume could be controlled accurately by the linear relationship between the waveform and the printed droplet volume [94]. In addition, some researchers quantified the influence of ink concentrations, voltage amplitude, dwell time and frequency on droplet diameter experimentally, and the modeling results can be used for precise control of the printed droplet size and shape [81, 95], but there is a need to take the process drifts and system variations into consideration to further improve the printing controllability.

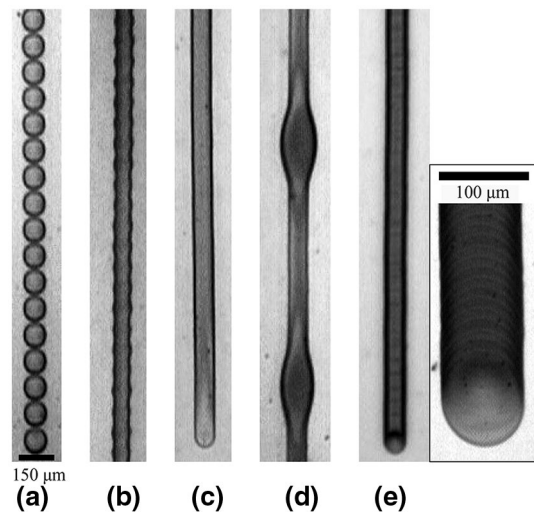


Fig. 5 Printed line morphology with respect to different droplet distance: **a** individual droplets, **b** scalloped line, **c** uniform line, **d** bulging line, and **e** stacked coins Reprinted with permission from ref. [50]. Copyright (2008) American Chemical Society

Different from the original application of IJP where the discrete droplets are printed for graphic output, conductive line is the basic element for inkjet-printed electronics, and the ideal lines should be printed smooth, even, and straight to enhance the electrical properties of a fabricated component. As the printed lines are produced by the coalescence of printed drops, the formation process from initial coalescence to solidification should be clearly understood, and the requirements that produce stable printed lines of spread droplets on a substrate can be considered as a crucial criterion for inkjet-printed lines. Soltman et al. [50] investigated the printed line morphologies by varying the combinations of drop spacing, drop delay and substrate temperature experimentally. The observations as shown in Fig. 5 demonstrated that the inkjet-printed line morphology could be influenced by the droplet distance significantly. Moreover, to ensure the MC for IJP, an operating window with respect to drop delay and drop spacing was proposed as qualitative guidance for fabricating uniform line.

To further improve the controllability on the printed line morphology, the stability of overlapping droplets and the subsequent formation process have been investigated theoretically. Davis investigated the stability of a liquid bead on a flat substrate subject to three constraint conditions on contact line and contact angle [96], and his predictions were confirmed by Schiaffino and Sonin experimentally [97]. Duineveld analyzed the behavior of inkjet-printed droplets by considering different substrates and contact angles and proposed a numerical model to predict the bulging instability with respect to droplet distance and the print speed. The proposed model indicated a maximum stable liquid bead

width that could be achieved through inkjet printing [98]. In addition, based on the volume conservation model, a lower bound to ensure a stable liquid line width was defined by Stringer and Derby [99]. And, then by combining with Duineveld's results, a stability model was proposed to define the upper and lower bounds of stable liquid beads by the droplet distance, the static advancing contact angle, and the print speed. Despite these limited bounds are beneficial to ensure the stability of inkjet-printed line, they are restricted to certain factors due to the complexity of droplets coalescence process. To fully explore the stability in a design space, it is advantageous to adopt a data-based approach to systematic investigate the interaction between substrate properties (temperature, wettability, roughness), physical parameters of the functional ink (surface tension, viscosity and density) and process parameters (droplet spacing, jetting delay, waveform, voltage). Recently, extensive researches have been reported on improving the printed line resolution by adjusting surface energy, ink concentration or modifying the surface topology [46, 82, 93, 99, 100]. However, the precise control of the printed line width is still required for inkjet-printed electronics to satisfy different engineering constraints. Although the MC could be achieved from empirical or theoretical models [101, 102], there is a lack of quantitative research on the printed line quality, and the model should be calibrated before use, if the system tends to drift during printing. Therefore, an in situ monitoring and online optimization approach is necessary to ensure a high controllability over the line morphology and printed line quality.

4.2 Aerosol Jet Printing Process

In comparison with IJP, despite AJP technology has higher ink printability, the printing process is more complex and the influencing factors remain a challenge to be controlled effectively. Among these factors, the key controllable variables of AJP are SHGFR, CGFR and print speed. As shown in Fig. 6, the printed line morphology with respect to adjustable parameters can be split into four major types [44, 47].

As the geometrical properties of the printed lines could affect the electrical properties significantly [43, 103, 104], most previous researches on improving line quality have been focused on the AJP process modeling and process parameter optimization to control the geometrical properties of the printed patterns. Several researchers proposed different criteria to identify operating windows for printing quality optimization. Mahajan et al. [44] studied the influence of SHGFR, CGFR and print speed on the line morphology, and an operating window was determined by experiments to print normal lines with higher thickness and less line width. Verheecke et al. [48], and Wang et al. [43] defined the edge roughness and extracted the printed lines morphology offline

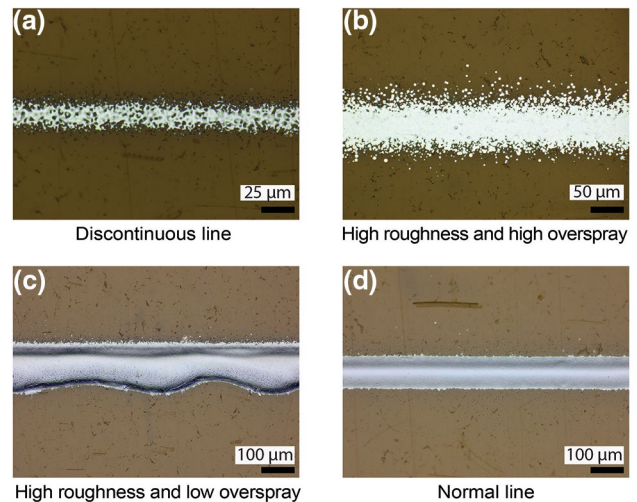


Fig. 6 Different printed line morphology in a design space. **a** A discontinuous line, **b** a high roughness and high overspray line, **c** a high roughness line, **d** a line printed under optimized conditions

for printing quality analysis, then a process window was developed to reduce the printed line edge roughness. Despite these operability windows were advantageous to optimize the printed line morphology, they were lacking quantitative description of the correlations between the adjustable factors and the line morphology. And the exploration in a design space was insufficient as the limited experimental design, thus it will be inefficient to adjust the process parameters for printing the customized line width, especially when there is a need to search for the universal 'optimal' process parameters in a design space for quality optimization [52].

To achieve better understanding on the process modeling of the AJP technology, many researchers have worked on elucidating aerosol transport and deposition mechanisms by mathematical models. Schulz et al. [105] proposed an analytical model to describe the discrete phase transported in a focused microcapillary. The modeling results showed that the Saffman force caused the aerosol flow to migrate radially inward at high velocities and the degree of collimation has been greatly improved at the nozzle exit. Akhatov et al. [106] further validated this phenomenon by considering Stokes drag force, Saffman force and particle inertia as the three main forces acted on particles in shear flow and analyzing the transport process of particle through long converging capillaries. The results also showed that the position and size of the atomized droplet in a shear gas flow had significant influence on the Saffman force. Based on the aerosol transport and deposition mechanisms, the relationship between process parameters and printed line geometry were explored by computational fluid dynamics (CFD) models. Salary et al. [47] formulated a simplified 2D-CFD model to elucidate the underlying aerodynamic

interaction between SHGFR and CGFR, thereby explaining the trends of printed line width with respect to SHGFR and CGFR. Hoey et al. [107] proposed a 3D-CFD model to describe aerosol transport mechanisms at the micron-scale. The results demonstrated that the specified geometry and flow characteristics had significant influence on Saffman force. Feng [108] developed a 3D-CFD model to evaluate the influence of the taper angle of the nozzle and working height on the deposition spot size. The CFD models which can be used to explain the specific aerodynamic interaction between different process factors are mainly determined by the individual AJP system and ink properties. Moreover, as AJP system tends to drift during printing as the influence of many changing and uncertain factors, the stationary CFD models may not suffice for quality control during the printing process. Hence, if a high controllability over the line morphology is required, it is necessary to adopt an in situ monitoring system for data-driven based process modeling [53, 104] and quantify the printed line morphology [43, 47, 109] for real time detection and quality optimization.

4.3 Printed Line Uniformity

Despite different printing principles are adopted to deposit drops on a substrate for fabricating conductive lines, the coffee-ring effect will inevitably occur in AJP and IJP. As shown in Fig. 7, the coffee-ring effect formed because of the non-uniform distribution of nanoparticles from the centers of the droplets to the edges.

As the ring-like morphology will affect the printed line uniformity and performance of patterned devices significantly, different techniques have been applied to control the coffee-ring effect [76]. Since the outward capillary flow transports the nanoparticles to the droplet edge and induces

the coffee ring effect, many groups have proposed to reduce the outward capillary flow by regulating the condition of solvent evaporation, such as employing the cooled substrate [50], raising the ambient humidity [65], introducing responsive materials [110, 111] and producing interactions among particles [112, 113]. On the other hand, as a Marangoni flow generally has an inward direction [66], researches have reported to produce the Marangoni flow to control the coffee-ring effect by adding compositional solvent [114], surfactants [77] and introducing a solvent surrounding [115]. Moreover, since a balance of droplet on the depinned substrate could be maintained by the sliding three phase contact line to help particles move inward, different substrate properties and receding contact angles were also investigated to improve the uniformity [116, 117]. Despite the above pre-processing approaches are beneficial to control the coffee-ring effect, they are highly dependent on the individual ink properties and lack of consideration for post-printing stage. Therefore, to improve the printed line uniformity, it is more important to optimize the sintering approach to reduce the coffee-ring effect in the post-processing stage.

5 In Situ Process Monitoring and Online Optimization of Non-contact Ink Writing Processes

Previous traditional approaches as discussed above were mainly restricted to identify the overall trend of the printing quality and optimize the printed features qualitatively in nature [44, 50, 52, 67]. Despite physics-based models were adopted to investigate the printing processes quantitatively [47, 84, 87, 108], they were highly dependent on an individual printing system and the limited computational resource hinders its practical applications in non-contact writing processes. To ensure sufficient process controllability and high printing accuracy of the non-contact ink writing processes, it is necessary to formulate a systematic mathematical model for a complete understanding of the printing process [53, 118]. Under such circumstances, different data-driven based approaches were proposed to model the quantitative correlations between the influencing factors and the printed features efficiently [53, 103, 104, 118–120]. Moreover, as the influence of many changing and uncertain factors during printing, such as material inhomogeneity, solvent evaporation, pressure and temperature fluctuations, the printing process (droplet behavior, line morphology) may drift with time and the inappropriate parameter settings will deteriorate the geometric features (width, thickness, roughness) and functional performance (conductivity, flexibility) of the fabricated components [121]. Therefore, in situ monitoring approaches were adopted in non-contact ink writing technologies to detect the process drifts and reduce material

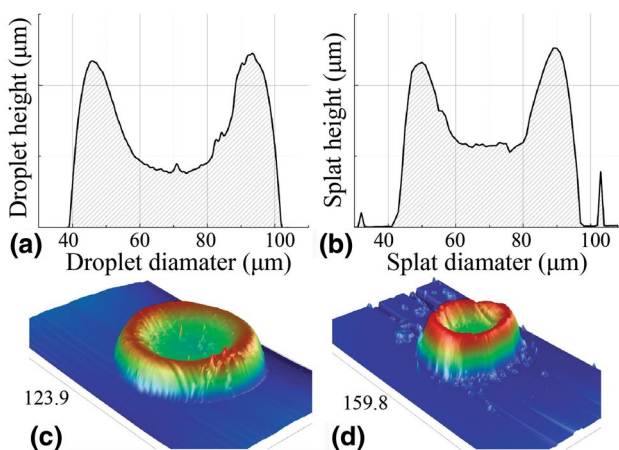


Fig. 7 a, c 2D and 3D profile of an inkjet-printed droplet, b, d 2D and 3D profile of an aerosol jet-printed droplet Adapted with permission from ref. [51]. Copyright (2015) American Chemical Society

waste during printing [103, 120–124]. Different from traditional post-process verification approaches, advances of the in situ monitoring approaches could assist not only in-process diagnosis for human-in-loop printing processes, they have the potential to integrate a closed-loop control system for real-time detection and online optimization of the non-contact ink writing processes [47, 118, 119, 125, 126]. Based on the integrated closed-loop control, controllable process parameters could be adjusted online to reduce the predicted defects, compensate the random variations, and ensure the process repeatability for the subsequent printing.

As shown in Fig. 8, an in situ monitoring and online optimization system for the non-contact writing processes is consisted of three main parts: (1) in situ monitoring, (2) data-driven based process modeling, (3) closed-loop feedback control [119, 125, 126]. Accordingly, the major challenges and requirements to bring in situ monitoring and online optimization technologies to a non-contact ink writing technology are as follows:

1. In situ monitoring. Image capturing and feature extraction are cores of the in situ monitoring system [127–130]. The basic elements (droplet diameter for IJP, line width for AJP) of non-contact ink writing technologies are fabricated in microns [51], which imposes the challenge to adopt an in situ monitoring system to accurately capture the printed features, particularly when the in situ monitoring system is required to be designed cost-effectively and deployed compactly [121]. Besides, the in situ monitoring system should have the capability of capturing the printing behaviors at high speed, which would be helpful to real-time printing process inspection and online optimization [121, 124]. Moreover, to fully analyze the printing behavior, it would be challenging to extract and recover critical multi-dimensional information from the incomplete information in reduced 2D space [119, 131].
2. Data driven-based modeling. Considering the high complexity and nonlinearity of the non-contact ink

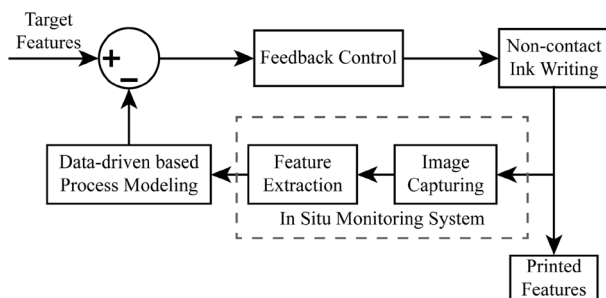


Fig. 8 Flowchart of an in situ monitoring and online optimization system in non-contact ink writing processes

writing processes, the data-driven based regression approaches are more suitable for modeling the printing process quantitatively [53, 118]. However, due to the drifting nature of the printing processes [52], the significant challenge is how to identify the main controllable parameters from various influencing factors, and model the printing process by a small data set rapidly and accurately [132, 133]. Moreover, to further enhance the modeling efficiency, there is a need to consider the similarity of the material deposition mechanism between different printing process, hence a novel printing process could be identified more efficiently based on the process similarity and model migration [134, 135].

3. Feedback control. As the data-driven based feedback control is extremely different from traditional model-driven based feedback control, it imposes challenges in ensuring the control stability of the non-contact ink writing processes while solving the complex non-linear control problems [136, 137]. Additionally, to reduce the produced defects and subsequent material waste during the control process, the designed controller should achieve the capability of fast convergence. Moreover, considering the drifting nature and system variations [47, 52, 70], there is a need to ensure the robustness of the designed controller, thus the process drifts could be corrected in real-time and the printing behavior is less sensitive to the changing uncontrollable factors [119].

Despite the real-time monitoring and online optimization of the non-contact ink writing processes has not been fully explored, different methods were proposed in recent years to address these major challenges. For IJP, the features of the droplets are extracted as essential for in-process diagnosis and online optimization. Wang et al. [122] proposed a computational light beam field based system to detect the location of droplets, hence the repeatability of the printing quality could be quantified and certified during the process. Kwon [124] demonstrated that by using a charge coupled device camera and the edge detection technology, the speed and size of droplets could be measured efficiently for in situ monitoring. Besides, a catadioptric stereo system was adopted to inspect the speed and location of 3D droplets with high accuracy and fast processing speed [121]. Based on the in situ monitoring technologies, Wu et al. [53] adopted an ensemble learning algorithm to predict the volume and velocity of single droplet, Wang et al. [119] modeled the relationship between the extracted droplet features and the labelled printing quality by a neural network, the modeling results demonstrated the effectiveness of the above data-driven based approaches. Additionally, to realize online optimization of the printing quality, a proportional-integral-derivative (PID) controller was integrated with the proposed neural network model to control the drive voltage to reduce

the defects induced by system variations, the experimental results validated the robustness of the adopted PID controller [119]. Despite the adopted approaches were beneficial to in situ monitoring and online optimization of the droplet behavior, it is necessary to further consider the coalescence process of droplets, which will be helpful to optimize the printed line quality of IJP.

On the other hand, as the deposition mechanism is different from IJP, the printed line features are usually extracted for real-time detection and online optimization of AJP process. To detect the incipient process drifts of AJP, Salary et al. [47] quantified the printed line morphology for in situ monitoring in the printing process, and a CFD model was adopted for determining the corrective action to bring the drifting process back in control. To achieve online assessment of the electrical properties, some researchers further investigated the correlations between the image-based line features and the printed line resistance. Sun et al. [104] studied the joint correlations of overspray and resistance based on the extracted features from microscopic images. Li et al. [120] proposed a spatial variable selection method to identify key image features from raw images for printed line resistance modeling. Salary et al. [103] recovered the cross-sectional profile of printed lines from the online images by shape-from-shading techniques, hence the line resistance could be evaluated for in situ monitoring. Despite the above studies revealed the potential relationships between in situ image-based line features and the electrical properties, it is necessary to further investigate the hierarchical relationships among process parameters, in situ line features and the electrical properties for AJP [118], thus the main process parameters could be considered as controllable variables for online morphology control and uniformity improvement of electrical performance [126].

6 Closing Remarks and Future Work

In this paper, we reviewed the state of art in quality optimization and precise control techniques that adopted in non-contact ink writing processes and discussed the advantages and disadvantages of the IJP and AJP techniques. From the literature review, the process parameters were regarded as the critical adjustable factors that could influence the printed line morphology. Although the traditional offline approaches were helpful to optimize the printing quality of non-contact ink writing processes, they were mainly restricted to identify the overall trend of the printing quality and optimize the printed features qualitatively in nature. As the printing process is very sensitive to the system drifts and random variations, if a high controllability over the printed line morphology is required, an in situ monitoring and online optimization system which consists of real time monitoring,

data-driven based process modeling and closed-loop feedback control is necessary to ensure the printing process remain stable. Despite the in situ process monitoring and online optimization system has the potential to detect system drifts, compensate the random variations and ensure the high controllability during the printing process, the following factors are involved to further develop the non-contact ink writing system: (1) combing the traditional operating windows with the in situ process monitoring and online optimization system to optimize the coalescence process of droplets and ensure the overall printed line quality, (2) modeling the hierarchical relationships among process parameters, in situ line features and the electrical properties to optimize the functional properties of fabricated components [118], (3) multi-objective optimization of the conflicting line features [30, 44, 48], such as a line could be fabricated with better aspect ratios (thickness/width), or customized line width printing with less roughness and overspray, and (4) developing a sintering approach to optimize the printed line uniformity of cross-sectional area in the post-processing stage [45, 51].

Acknowledgements This research work was conducted in the SMRT-NTU Smart Urban Rail Corporate Laboratory with funding support from the National Research Foundation (NRF), SMRT and Nanyang Technological University; under the Corp Lab@University Scheme.

References

1. Han, T.-H., Lee, Y., Choi, M.-R., Woo, S.-H., Bae, S.-H., et al. (2012). Extremely efficient flexible organic light-emitting diodes with modified graphene anode. *Nature Photonics*, 6(2), 105.
2. Zhu, H., Xiao, Z., Liu, D., Li, Y., Weadock, N. J., et al. (2013). Biodegradable transparent substrates for flexible organic-light-emitting diodes. *Energy and Environmental Science*, 6(7), 2105–2111.
3. Krebs, F. C. (2009). Fabrication and processing of polymer solar cells: a review of printing and coating techniques. *Solar Energy Materials and Solar Cells*, 93(4), 394–412.
4. Thompson, B. C., & Fréchet, J. M. (2008). Polymer–fullerene composite solar cells. *Angewandte Chemie International Edition*, 47(1), 58–77.
5. Jung, M., Kim, J., Noh, J., Lim, N., Lim, C., et al. (2010). All-printed and roll-to-roll-printable 13.56-MHz-operated 1-bit RF tag on plastic foils. *IEEE Transactions on Electron Devices*, 57(3), 571–580.
6. Zheng, Y., He, Z., Gao, Y., & Liu, J. (2013). Direct desktop printed-circuits-on-paper flexible electronics. *Scientific reports*, 3, 1786.
7. Kim, T.-I., Hwan Jung, Y., Chung, H.-J., Jun Yu, K., Ahmed, N., et al. (2013). Deterministic assembly of releasable single crystal silicon-metal oxide field-effect devices formed from bulk wafers. *Applied Physics Letters*, 102(18), 182104.
8. Clemens, W., Fix, W., Ficker, J., Knobloch, A., & Ullmann, A. (2004). From polymer transistors toward printed electronics. *Journal of Materials Research*, 19(7), 1963–1973.
9. Yan, H., Chen, Z., Zheng, Y., Newman, C., Quinn, J. R., et al. (2009). A high-mobility electron-transporting polymer for printed transistors. *Nature*, 457(7230), 679.

10. Chang, W.-Y., Fang, T.-H., Lin, H.-J., Shen, Y.-T., & Lin, Y.-C. (2009). A large area flexible array sensors using screen printing technology. *Journal of display technology*, 5(6), 178–183.
11. Khan, S., Lorenzelli, L., & Dahiya, R. (2014). Bendable piezoresistive sensors by screen printing MWCNT/PDMS composites on flexible substrates. 10th Conference on Ph. D. Research in Microelectronics and Electronics, France.
12. Qi, Q., Zhang, T., Yu, Q., Wang, R., Zeng, Y., et al. (2008). Properties of humidity sensing ZnO nanorods-base sensor fabricated by screen-printing. *Sensors and Actuators B: Chemical*, 133(2), 638–643.
13. Kim, K., Kim, J., Kim, B., & Ko, S. (2018). Fabrication of microfluidic structure based biosensor using roll-to-roll gravure printing. *International Journal of Precision Engineering and Manufacturing-Green Technology*, 5(3), 369–374.
14. Jeong, T.-G., Seo, Y.-H., Kim, S., Song, J., Ko, S.-L., et al. (2014). Roll to roll air-floating oven drying process design and analysis for printed electronics. *International Journal of Precision Engineering and Manufacturing*, 15(7), 1303–1310.
15. Chu, W.-S., Kim, C.-S., Lee, H.-T., Choi, J.-O., Park, J.-I., et al. (2014). Hybrid manufacturing in micro/nano scale: a review. *International Journal of Precision Engineering and Manufacturing-Green Technology*, 1(1), 75–92.
16. Pease, R. F., & Chou, S. Y. (2008). Lithography and other patterning techniques for future electronics. *Proceedings of the IEEE*, 96(2), 248–270.
17. Søndergaard, R. R., Hösel, M., & Krebs, F. C. (2013). Roll-to-roll fabrication of large area functional organic materials. *Journal of Polymer Science Part B: Polymer Physics*, 51(1), 16–34.
18. Nathan, A., Ahnood, A., Cole, M. T., Lee, S., Suzuki, Y., et al. (2012). Flexible electronics: the next ubiquitous platform. *Proceedings of the IEEE*, 100, 1486–1517.
19. Yoon, H.-S., Lee, J.-Y., Kim, H.-S., Kim, M.-S., Kim, E.-S., et al. (2014). A comparison of energy consumption in bulk forming, subtractive, and additive processes: Review and case study. *International Journal of Precision Engineering and Manufacturing-Green Technology*, 1(3), 261–279.
20. Sharma, A., Mondal, S., Mondal, A. K., Baksi, S., Patel, R. K., et al. (2017). 3D printing: It's microfluidic functions and environmental impacts. *International Journal of Precision Engineering and Manufacturing-Green Technology*, 4(3), 323–334.
21. Khan, S., Lorenzelli, L., & Dahiya, R. (2014). Technologies for printing sensors and electronics over large flexible substrates: a review. *IEEE Sensors Journal*, 15(6), 3164–3185.
22. Hon, K., Li, L., & Hutchings, I. (2008). Direct writing technology—Advances and developments. *CIRP Annals*, 57(2), 601–620.
23. Kang, M., & Kang, K.-T. (2018). Flexible 2-layer paper printed circuit board fabricated by inkjet printing for 3-D origami electronics. *International Journal of Precision Engineering and Manufacturing-Green Technology*, 5(3), 421–426.
24. Sung, K.-H., Park, J., & Kang, H. (2018). Multi-layer inkjet printing of Ag nanoparticle inks and its sintering with a near-infrared system. *International Journal of Precision Engineering and Manufacturing*, 19(2), 303–307.
25. Jang, S. H., Oh, S. T., Lee, I. H., Kim, H.-C., & Cho, H. Y. (2015). 3-Dimensional circuit device fabrication process using stereolithography and direct writing. *International Journal of Precision Engineering and Manufacturing*, 16(7), 1361–1367.
26. Braga, D., Erickson, N. C., Renn, M. J., Holmes, R. J., & Frisbie, C. D. (2012). High-transconductance organic thin-film electrochemical transistors for driving low-voltage red–green–blue active matrix organic light-emitting devices. *Advanced Functional Materials*, 22(8), 1623–1631.
27. Hong, K., Kim, S. H., Mahajan, A., & Frisbie, C. D. (2014). Aerosol jet printed p-and n-type electrolyte-gated transistors with a variety of electrode materials: exploring practical routes to printed electronics. *ACS Applied Materials and Interfaces*, 6(21), 18704–18711.
28. Mauthner, G., Landfester, K., Köck, A., Brückl, H., Kast, M., et al. (2008). Inkjet printed surface cell light-emitting devices from a water-based polymer dispersion. *Organic Electronics*, 9(2), 164–170.
29. Shimoda, T., Morii, K., Seki, S., & Kiguchi, H. (2003). Inkjet printing of light-emitting polymer displays. *MRS Bulletin*, 28(11), 821–827.
30. Tait, J. G., Witkowska, E., Hirade, M., Ke, T.-H., Malinowski, P. E., et al. (2015). Uniform Aerosol Jet printed polymer lines with 30 μm width for 140 ppi resolution RGB organic light emitting diodes. *Organic Electronics*, 22, 40–43.
31. Crowley, K., O'Malley, E., Morrin, A., Smyth, M. R., & Killard, A. J. (2008). An aqueous ammonia sensor based on an inkjet-printed polyaniline nanoparticle-modified electrode. *Analyst*, 133(3), 391–399.
32. Jang, J., Ha, J., & Cho, J. (2007). Fabrication of water-dispersible polyaniline-poly (4-styrenesulfonate) nanoparticles for inkjet-printed chemical-sensor applications. *Advanced Materials*, 19(13), 1772–1775.
33. Böberl, M., Kovalenko, M. V., Gamerith, S., List, E. J., & Heiss, W. (2007). Inkjet-printed nanocrystal photodetectors operating up to 3 μm wavelengths. *Advanced Materials*, 19(21), 3574–3578.
34. Zhao, D., Liu, T., Zhang, M., Liang, R., & Wang, B. (2012). Fabrication and characterization of aerosol-jet printed strain sensors for multifunctional composite structures. *Smart Materials and Structures*, 21(11), 115008.
35. Hoth, C. N., Choulis, S. A., Schilinsky, P., & Brabec, C. J. (2007). High photovoltaic performance of inkjet printed polymer: fullerene blends. *Advanced Materials*, 19(22), 3973–3978.
36. Contreras, M. A., Ramanathan, K., AbuShama, J., Hasoon, F., Young, D. L., et al. (2005). ACCELERATED PUBLICATION: Diode characteristics in state-of-the-art ZnO/CdS/Cu (In1-xGax) Se2 solar cells. *Progress in Photovoltaics: Research and Applications*, 13(3), 209–216.
37. Kopola, P., Zimmermann, B., Filipovic, A., Schleiermacher, H.-F., Greulich, J., et al. (2012). Aerosol jet printed grid for ITO-free inverted organic solar cells. *Solar Energy Materials and Solar Cells*, 107, 252–258.
38. Ou, C., Sangle, A. L., Datta, A., Jing, Q., Busolo, T., et al. (2018). Fully printed organic-inorganic nanocomposites for flexible thermoelectric applications. *ACS Applied Materials & Interfaces*, 10(23), 19580–19587.
39. Lee, J., Kim, H.-C., Choi, J.-W., & Lee, I. H. (2017). A review on 3D printed smart devices for 4D printing. *International Journal of Precision Engineering and Manufacturing-Green Technology*, 4(3), 373–383.
40. Kwon, J., Park, H. W., Park, Y.-B., & Kim, N. (2017). Potentials of additive manufacturing with smart materials for chemical biomarkers in wearable applications. *International Journal of Precision Engineering and Manufacturing-Green Technology*, 4(3), 335–347.
41. Kim, M.-S., Chu, W.-S., Kim, Y.-M., Avila, A. P. G., & Ahn, S.-H. (2009). Direct metal printing of 3D electrical circuit using rapid prototyping. *International journal of Precision Engineering and Manufacturing*, 10(5), 147–150.
42. Ahn, D.-G. (2016). Direct metal additive manufacturing processes and their sustainable applications for green technology: A review. *International Journal of Precision Engineering and Manufacturing-Green Technology*, 3(4), 381–395.
43. Wang, K., Chang, Y.-H., Zhang, C., & Wang, B. (2013). Evaluation of quality of printed strain sensors for composite structural

- health monitoring applications. In *SAMPE fall technical conference*, USA.
44. Mahajan, A., Frisbie, C. D., & Francis, L. F. (2013). Optimization of aerosol jet printing for high-resolution, high-aspect ratio silver lines. *ACS Applied Materials and Interfaces*, *5*(11), 4856–4864.
 45. Kim, C., Nogi, M., & Sukanuma, K. (2012). Electrical conductivity enhancement in inkjet-printed narrow lines through gradual heating. *Journal of Micromechanics and Microengineering*, *22*(3), 035016.
 46. Doggart, J., Wu, Y., & Zhu, S. (2009). Inkjet printing narrow electrodes with <math>< 50 \mu\text{m}</math> line width and channel length for organic thin-film transistors. *Applied Physics Letters*, *94*(16), 163503.
 47. Salary, R. R., Lombardi, J. P., Tootooni, M. S., Donovan, R., Rao, P. K., et al. (2017). Computational fluid dynamics modeling and online monitoring of aerosol jet printing process. *Journal of Manufacturing Science and Engineering*, *139*(2), 021015.
 48. Verheecke, W., Van Dyck, M., Vogeler, F., Voet, A., & Valkenaers, H. (2012). Optimizing aerosol jet printing of silver interconnects on polyimide film for embedded electronics applications. In *Eighth international DAAAM baltic conference industrial engineering*, Estonia.
 49. Oh, Y., Kim, J., Yoon, Y. J., Kim, H., Yoon, H. G., et al. (2011). Inkjet printing of Al_2O_3 dots, lines, and films: From uniform dots to uniform films. *Current Applied Physics*, *11*(3), S359–S363.
 50. Soltman, D., & Subramanian, V. (2008). Inkjet-printed line morphologies and temperature control of the coffee ring effect. *Langmuir*, *24*(5), 2224–2231.
 51. Seifert, T., Sowade, E., Roscher, F., Wiemer, M., Gessner, T., et al. (2015). Additive manufacturing technologies compared: morphology of deposits of silver ink using inkjet and aerosol jet printing. *Industrial and Engineering Chemistry Research*, *54*(2), 769–779.
 52. Smith, M., Choi, Y. S., Boughey, C., & Kar-Narayan, S. (2017). Controlling and assessing the quality of aerosol jet printed features for large area and flexible electronics. *Flexible and Printed Electronics*, *2*(1), 015004.
 53. Wu, D., & Xu, C. (2018). Predictive modeling of droplet formation processes in inkjet-based bioprinting. *Journal of Manufacturing Science and Engineering*, *140*(10), 101007.
 54. Rahman, K., Khan, A., Nam, N. M., Choi, K. H., & Kim, D.-S. (2011). Study of drop-on-demand printing through multi-step pulse voltage. *International Journal of Precision Engineering and Manufacturing*, *12*(4), 663–669.
 55. Lim, T., Yang, J., Lee, S., Chung, J., & Hong, D. (2012). Deposit pattern of inkjet printed pico-liter droplet. *International Journal of Precision Engineering and Manufacturing*, *13*(6), 827–833.
 56. Yang, Y. J., Kim, H. C., Sajid, M., Kim, S. W., Aziz, S., et al. (2018). Drop-on-demand electrohydrodynamic printing of high resolution conductive micro patterns for MEMS repairing. *International Journal of Precision Engineering and Manufacturing*, *19*(6), 811–819.
 57. Tan, H., Tran, T., & Chua, C. (2016). A review of printed passive electronic components through fully additive manufacturing methods. *Virtual and Physical Prototyping*, *11*(4), 271–288.
 58. Cruz, S. M. F., Rocha, L. A., & Viana, J. C. (2018). *Printing technologies on flexible substrates for printed electronics, in flexible electronics*. London: IntechOpen.
 59. Nir, M. M., Zamir, D., Haymov, I., Ben-Asher, L., Cohen, O., et al. (2010). Electrically conductive inks for inkjet printing. *the chemistry of inkjet inks* (pp. 225–254). Singapore: World Scientific.
 60. King, B. H., O'Reilly, M. J., & Barnes, S.M. (2009). Characterizing aerosol Jet[®] multi-nozzle process parameters for non-contact front side metallization of silicon solar cells. In *34th IEEE photovoltaic specialists conference*, USA.
 61. Cai, F., Pavlidis, S., Papapolymerou, J., Chang, Y. H., Wang, K. et al. (2014). Aerosol jet printing for 3-D multilayer passive microwave circuitry. In *44th European microwave conference*, Italy.
 62. Goth, C., Putzo, S., & Franke, J. (2011). Aerosol Jet printing on rapid prototyping materials for fine pitch electronic applications. In *61st electronic components and technology conference*, USA.
 63. Paulsen, J. A., Renn, M., Christenson, K., & Plourde, R. (2012). Printing conformal electronics on 3D structures with aerosol jet technology. In *2012 future of instrumentation international workshop proceedings*, USA.
 64. Sridhar, A., Blaudeck, T., & Baumann, R. R. (2011). Inkjet printing as a key enabling technology for printed electronics. *Material Matters*, *6*(1), 12–15.
 65. Fukuda, K., Sekine, T., Kumaki, D., & Tokito, S. (2013). Profile control of inkjet printed silver electrodes and their application to organic transistors. *ACS Applied Materials and Interfaces*, *5*(9), 3916–3920.
 66. Ristenpart, W., Kim, P., Domingues, C., Wan, J., & Stone, H. (2007). Influence of substrate conductivity on circulation reversal in evaporating drops. *Physical Review Letters*, *99*(23), 234502.
 67. Derby, B. (2010). Inkjet printing of functional and structural materials: fluid property requirements, feature stability, and resolution. *Annual Review of Materials Research*, *40*, 395–414.
 68. Jang, D., Kim, D., & Moon, J. (2009). Influence of fluid physical properties on ink-jet printability. *Langmuir*, *25*(5), 2629–2635.
 69. Son, Y., Kim, C., Yang, D. H., & Ahn, D. J. (2008). Spreading of an inkjet droplet on a solid surface with a controlled contact angle at low Weber and Reynolds numbers. *Langmuir*, *24*(6), 2900–2907.
 70. Perelaer, J., Smith, P. J., Wijnen, M. M., van den Bosch, E., Eckardt, R., et al. (2009). Droplet tailoring using evaporative inkjet printing. *Macromolecular Chemistry and Physics*, *210*(5), 387–393.
 71. Liu, Y.-F., Tsai, M.-H., Pai, Y.-F., & Hwang, W.-S. (2013). Control of droplet formation by operating waveform for inks with various viscosities in piezoelectric inkjet printing. *Applied Physics A*, *111*(2), 509–516.
 72. Du, Z., Lin, Y., Xing, R., Cao, X., Yu, X., et al. (2018). Controlling the polymer ink's rheological properties and viscoelasticity to suppress satellite droplets. *Polymer*, *138*, 75–82.
 73. Kang, B. J., & Oh, J. H. (2010). Geometrical characterization of inkjet-printed conductive lines of nanosilver suspensions on a polymer substrate. *Thin Solid Films*, *518*(10), 2890–2896.
 74. Chouiki, M., & Schoeffner, R. (2011). Inkjet printing of inorganic sol-gel ink and control of the geometrical characteristics. *Journal of Sol-Gel Science and Technology*, *58*(1), 91–95.
 75. Wang, C., Hopkins, S. C., Tomov, R. I., Kumar, R. V., & Glowacki, B. A. (2012). Optimisation of CGO suspensions for inkjet-printed SOFC electrolytes. *Journal of the European Ceramic Society*, *32*(10), 2317–2324.
 76. Sun, J., Bao, B., He, M., Zhou, H., & Song, Y. (2015). Recent advances in controlling the depositing morphologies of inkjet droplets. *ACS Applied Materials and Interfaces*, *7*(51), 28086–28099.
 77. Kajiya, T., Kobayashi, W., Okuzono, T., & Doi, M. (2009). Controlling the drying and film formation processes of polymer solution droplets with addition of small amount of surfactants. *The Journal of Physical Chemistry B*, *113*(47), 15460–15466.
 78. Yang, L., Kapur, N., Wang, Y., Fiesser, F., Bierbrauer, F., et al. (2018). Drop-on-demand satellite-free drop formation for precision fluid delivery. *Chemical Engineering Science*, *186*, 102–115.
 79. Shin, P., Sung, J., & Lee, M. H. (2011). Control of droplet formation for low viscosity fluid by double waveforms applied

- to a piezoelectric inkjet nozzle. *Microelectronics Reliability*, 51(4), 797–804.
80. Gan, H., Shan, X., Eriksson, T., Lok, B., & Lam, Y. (2009). Reduction of droplet volume by controlling actuating waveforms in inkjet printing for micro-pattern formation. *Journal of Micromechanics and Microengineering*, 19(5), 055010.
 81. Gao, Q., He, Y., Fu, J.-Z., Qiu, J.-J., & Jin, Y.-A. (2016). Fabrication of shape controllable alginate microparticles based on drop-on-demand jetting. *Journal of Sol-Gel Science and Technology*, 77(3), 610–619.
 82. Van Osch, T. H., Perelaer, J., de Laat, A. W., & Schubert, U. S. (2008). Inkjet printing of narrow conductive tracks on untreated polymeric substrates. *Advanced Materials*, 20(2), 343–345.
 83. Park, Y.-W., Oh, O.-K., & Noh, M. D. (2015). Ejection feasibility of high viscosity fluid with magnetostrictive inkjet printhead. *International Journal of Precision Engineering and Manufacturing*, 16(7), 1369–1374.
 84. Fromm, J. (1984). Numerical calculation of the fluid dynamics of drop-on-demand jets. *IBM Journal of Research and Development*, 28(3), 322–333.
 85. Reis, N., & Derby, B. (2000). Ink jet deposition of ceramic suspensions: Modeling and experiments of droplet formation. *MRS Online Proceedings Library Archive*, 625, 117–122.
 86. Szczech, J. B., Megaridis, C. M., Gamota, D. R., & Zhang, J. (2002). Fine-line conductor manufacturing using drop-on demand PZT printing technology. *IEEE Transactions on Electronics Packaging Manufacturing*, 25(1), 26–33.
 87. Wu, H.-C., Hwang, W.-S., & Lin, H.-J. (2004). Development of a three-dimensional simulation system for micro-inkjet and its experimental verification. *Materials Science and Engineering A*, 373(1–2), 268–278.
 88. De Gans, B. J., Duineveld, P. C., & Schubert, U. S. (2004). Inkjet printing of polymers: state of the art and future developments. *Advanced Materials*, 16(3), 203–213.
 89. Dong, H., Carr, W. W., & Morris, J. F. (2006). An experimental study of drop-on-demand drop formation. *Physics of Fluids*, 18(7), 072102.
 90. Seerden, K. A., Reis, N., Evans, J. R., Grant, P. S., Halloran, J. W., et al. (2001). Ink-jet printing of wax-based alumina suspensions. *Journal of the American Ceramic Society*, 84(11), 2514–2520.
 91. Jo, B. W., Lee, A., Ahn, K. H., & Lee, S. J. (2009). Evaluation of jet performance in drop-on-demand (DOD) inkjet printing. *Korean Journal of Chemical Engineering*, 26(2), 339–348.
 92. Wilson, P., Lekakou, C., & Watts, J. (2014). System design and process optimization for the inkjet printing of PEDOT: Poly (styrenesulfonate). *Journal of Micro and Nano-Manufacturing*, 2(1), 011004.
 93. Wu, J.-T., Hsu, S. L.-C., Tsai, M.-H., & Hwang, W.-S. (2010). Direct inkjet printing of silver nitrate/poly (*N*-vinyl-2-pyrrolidone) inks to fabricate silver conductive lines. *The Journal of Physical Chemistry C*, 114(10), 4659–4662.
 94. Chen, F., Zhang, Y., Nakagawa, Y., Zeng, H., Luo, C., et al. (2013). A piezoelectric drop-on-demand generator for accurate samples in capillary electrophoresis. *Talanta*, 107, 111–117.
 95. Herran, C. L., & Huang, Y. (2012). Alginate microsphere fabrication using bipolar wave-based drop-on-demand jetting. *Journal of manufacturing processes*, 14(2), 98–106.
 96. Davis, S. H. (1980). Moving contact lines and rivulet instabilities. Part 1. The static rivulet. *Journal of Fluid Mechanics*, 98(2), 225–242.
 97. Schiaffino, S., & Sonin, A. A. (1997). Formation and stability of liquid and molten beads on a solid surface. *Journal of fluid mechanics*, 343, 95–110.
 98. Duineveld, P. C. (2003). The stability of ink-jet printed lines of liquid with zero receding contact angle on a homogeneous substrate. *Journal of Fluid Mechanics*, 477, 175–200.
 99. Stringer, J., & Derby, B. (2009). Limits to feature size and resolution in ink jet printing. *Journal of the European Ceramic Society*, 29(5), 913–918.
 100. Kuang, M., Wang, L., & Song, Y. (2014). Controllable printing droplets for high-resolution patterns. *Advanced Materials*, 26(40), 6950–6958.
 101. Smith, P., Shin, D.-Y., Stringer, J., Derby, B., & Reis, N. (2006). Direct ink-jet printing and low temperature conversion of conductive silver patterns. *Journal of Materials Science*, 41(13), 4153–4158.
 102. Wu, J.-T., Hsu, S. L.-C., Tsai, M.-H., & Hwang, W.-S. (2011). Inkjet printing of low-temperature cured silver patterns by using AgNO₃/1-dimethylamino-2-propanol inks on polymer substrates. *The Journal of Physical Chemistry C*, 115(22), 10940–10945.
 103. Salary, R. R., Lombardi, J. P., Rao, P. K., & Poliks, M. D. (2017). Online monitoring of functional electrical properties in aerosol jet printing additive manufacturing process using shape-from-shading image analysis. *Journal of Manufacturing Science and Engineering*, 139(10), 101010.
 104. Sun, H., Wang, K., Li, Y., Zhang, C., & Jin, R. (2017). Quality modeling of printed electronics in aerosol jet printing based on microscopic images. *Journal of Manufacturing Science and Engineering*, 139(7), 071012.
 105. Schulz, D., Hoey, J., Thompson, D., Swenson, O., Han, S., et al. (2010). Collimated aerosol beam deposition: Sub-5- μ m resolution of printed actives and passives. *IEEE Transactions on Advanced Packaging*, 33(2), 421–427.
 106. Akhatov, I. S., Hoey, J. M., Thompson, D., Lutfurakhmanov, A., Mahmud, Z. et al. (2009). Aerosol flow through a micro-capillary. In *ASME second international conference on micro/nanoscale heat and mass transfer*, China.
 107. Hoey, J., Lutfurakhmanov, A., Robinson, M., Swenson, O., & Schulz, D. (2012). Advances in aerosol direct-write technology for fine line applications. In *ASME international mechanical engineering congress and exposition*, USA.
 108. Feng, J. Q. (2017). A computational study of particle deposition patterns from a circular laminar jet. *Journal of Applied Fluid Mechanics*, 10(4), 1001–1012.
 109. Huang, B.-C., Chan, H.-J., Hong, J.-W., & Lo, C.-Y. (2016). Methodology for evaluating pattern transfer completeness in inkjet printing with irregular edges. *Journal of Micromechanics and Microengineering*, 26(6), 065009.
 110. Anyfantakis, M., Geng, Z., Morel, M., Rudiuk, S., & Baigl, D. (2015). Modulation of the coffee-ring effect in particle/surfactant mixtures: the importance of particle–interface interactions. *Langmuir*, 31(14), 4113–4120.
 111. Anyfantakis, M., & Baigl, D. (2014). Dynamic photocontrol of the coffee-ring effect with optically tunable particle stickiness. *Angewandte Chemie*, 126(51), 14301–14305.
 112. Zhang, Y., Yang, S., Chen, L., & Evans, J. (2008). Shape changes during the drying of droplets of suspensions. *Langmuir*, 24(8), 3752–3758.
 113. Zhang, Y., & Evans, J. R. (2013). Morphologies developed by the drying of droplets containing dispersed and aggregated layered double hydroxide platelets. *Journal of colloid and interface science*, 395, 11–17.
 114. Wang, L., Wang, J., Huang, Y., Liu, M., Kuang, M., et al. (2012). Inkjet printed colloidal photonic crystal microdot with fast response induced by hydrophobic transition of poly (*N*-isopropyl acrylamide). *Journal of Materials Chemistry*, 22(40), 21405–21411.
 115. Majumder, M., Rendall, C. S., Eukel, J. A., Wang, J. Y., Behabtu, N., et al. (2012). Overcoming the “coffee-stain” effect by

- compositional Marangoni-flow-assisted drop-drying. *The Journal of Physical Chemistry B*, 116(22), 6536–6542.
116. Bao, B., Li, M., Li, Y., Jiang, J., Gu, Z., et al. (2015). Patterning fluorescent quantum dot nanocomposites by reactive inkjet printing. *Small (Weinheim an der Bergstrasse, Germany)*, 11(14), 1649–1654.
 117. Lessing, J., Glavan, A. C., Walker, S. B., Keplinger, C., Lewis, J. A., et al. (2014). Inkjet Printing of conductive inks with high lateral resolution on omniphobic “Rf paper” for paper-based electronics and MEMS. *Advanced Materials*, 26(27), 4677–4682.
 118. Li, Y., Mohan, K., Sun, H., & Jin, R. (2017). Ensemble modeling of in situ features for printed electronics manufacturing with in situ process control potential. *IEEE Robotics and Automation Letters*, 2(4), 1864–1870.
 119. Wang, T., Kwok, T.-H., Zhou, C., & Vader, S. (2018). In-situ droplet inspection and closed-loop control system using machine learning for liquid metal jet printing. *Journal of manufacturing systems*, 47, 83–92.
 120. Li, Y., Sun, H., Deng, X., Zhang, C., Wang, H.-P., et al. (2019). Manufacturing quality prediction using smooth spatial variable selection estimator with applications in Aerosol Jet[®] printed electronics manufacturing. *IIEE Transactions*, Accepted, pp. 1–17
 121. Wang, T., Zhou, C., & Xu, W. (2019). Online droplet monitoring in inkjet 3D printing using catadioptric stereo system. *IIEE Transactions*, 51(2), 153–167.
 122. Wang, A., Wang, T., Zhou, C., & Xu, W. (2017). LuBan: Low-cost and in situ droplet micro-sensing for inkjet 3D printing quality assurance. In *Proceedings of the 15th ACM conference on embedded network sensor systems*, USA.
 123. Lies, B. T., Cai, Y., Spahr, E., Lin, K., & Qin, H. (2018). Machine vision assisted micro-filament detection for real-time monitoring of electrohydrodynamic inkjet printing. *Procedia Manufacturing*, 26, 29–39.
 124. Kwon, K.-S. (2009). Speed measurement of ink droplet by using edge detection techniques. *Measurement*, 42(1), 44–50.
 125. Nguyen, T. K., Nguyen, V. D., Seong, B., Hoang, N., Park, J., et al. (2014). Control and improvement of jet stability by monitoring liquid meniscus in electrospray and electrohydrodynamic jet. *Journal of Aerosol Science*, 71, 29–39.
 126. Lombardi, J. P., Salary, R.R., Weerawarne, D.L., Rao, P.K. & Poliks, M.D. (2018). In-situ image-based monitoring and closed-loop control of aerosol jet printing. In *ASME 13th international manufacturing science and engineering conference*, USA.
 127. Park, J.-K., Kwon, B.-K., Park, J.-H., & Kang, D.-J. (2016). Machine learning-based imaging system for surface defect inspection. *International Journal of Precision Engineering and Manufacturing-Green Technology*, 3(3), 303–310.
 128. Seong, J., Kim, S., Park, J., Lee, D., & Shin, K.-H. (2015). Online noncontact thickness measurement of printed conductive silver patterns in roll-to-roll gravure printing. *International Journal of Precision Engineering and Manufacturing*, 16(11), 2265–2270.
 129. Kim, J. S., Lee, C. S., Kim, S.-M., & Lee, S. W. (2018). Development of data-driven in-situ monitoring and diagnosis system of fused deposition modeling (FDM) process based on support vector machine algorithm. *International Journal of Precision Engineering and Manufacturing-Green Technology*, 5(4), 479–486.
 130. Chua, Z. Y., Ahn, I. H., & Moon, S. K. (2017). Process monitoring and inspection systems in metal additive manufacturing: Status and applications. *International Journal of Precision Engineering and Manufacturing-Green Technology*, 4(2), 235–245.
 131. Kwon, K.-S., Go, J.-K., Kim, J.-W. & Oh, D. (2010). In situ measurement of instantaneous jetting speed curve. In *NIP & digital fabrication conference*, USA.
 132. Rasmussen, C. E. (1999). *Evaluation of Gaussian processes and other methods for non-linear regression*. Toronto: University of Toronto.
 133. Yuan, J., Wang, K., Yu, T., & Fang, M. (2008). Reliable multi-objective optimization of high-speed WEDM process based on Gaussian process regression. *International Journal of Machine Tools and Manufacture*, 48(1), 47–60.
 134. Pan, S. J., & Yang, Q. (2010). A survey on transfer learning. *IEEE Transactions on Knowledge and Data Engineering*, 22(10), 1345–1359.
 135. Luo, L., Yao, Y., & Gao, F. (2015). Bayesian improved model migration methodology for fast process modeling by incorporating prior information. *Chemical Engineering Science*, 134, 23–35.
 136. Hou, Z.-S., & Wang, Z. (2013). From model-based control to data-driven control: Survey, classification and perspective. *Information Sciences*, 235, 3–35.
 137. Formentin, S., Van Heusden, K., & Karimi, A. (2014). A comparison of model-based and data-driven controller tuning. *International Journal of Adaptive Control and Signal Processing*, 28(10), 882–897.

Publisher's Note Springer Nature remains neutral with regard to jurisdictional claims in published maps and institutional affiliations.



Haining Zhang is currently pursuing his Ph.D. under the supervision of Assistant Professor Seung Ki Moon at Nanyang Technological University (NTU), Singapore. His current research interests include data-driven based modeling, multi-objective optimization and uncertainty quantification of additive manufacturing processes.



Seung Ki Moon is an assistant professor in School of Mechanical and Aerospace Engineering, Nanyang Technological University, Singapore. He received his Ph.D. degree in Industrial Engineering from the Pennsylvania State University, USA, in 2008, his M.S. and B.S. degrees in Industrial Engineering from Hanyang University, S. Korea, in 1995 and 1992, respectively. He worked as a Senior Research Engineer at the Hyundai Motor Company, S. Korea for eight years before embarking on his

PhD degree. After completing his doctoral degree, he joined the Department of Mechanical Engineering, Texas A&M University for one year as a postdoctoral research associate. He is interested in the boundary-spanning research that integrates the knowledge of design, engineering, and economics. His current focuses include applying sciences and economic theory to the design of customized and sustainable products, services and systems, strategic and multidisciplinary design optimization, advanced modeling and simulation, design for additive manufacturing/3D printing, embedded sensor design for 3D Printing, smart factory, and redesign and remanufacturing for green technologies.



Teck Hui Ngo is the Head of Rolling Stock Engineering, SMRT Trains Pte Ltd, Singapore. As part of the SMRT-NTU Corporation Laboratory, he is the project representative from SMRT, working with Dr Seung Ki Moon on the development of customized 3D printed sensors for use on rolling stock equipment. He received his Bachelor of Engineering (Mechanical Engineering) from Nanyang Technological University and his Masters of Science (Industrial and Systems Engineering) from National University of Singapore.

He is actively looking at adopting new technology to improve the safety and reliability of rolling stock.